# Bayesian method in optical emission spectroscopy: evaluation of $n_e(t)$ from time-integrated $H_\alpha$ and validation with time-resolved measurements

A. Dorval[1] , R. Boumris[1], A. Hamdan[1], and L. Stafford[1]

[1] *Groupe de physique des plasmas, Département de Physique, Université de Montréal, Québec, Canada*

**Abstract:** In-liquid spark discharge is a promising field for many applications. The physics of the involved processes is far to be understood. The temporal evolution of the plasma properties is fast (~ns), which makes the measurement and the interpretation of the data a challenge. Here, we apply Bayesian method to exploit time-integrated Hα line emission intensities to derive time-resolved properties. The model predicted with high accuracy the line profile, and the properties (here $n_e(t)$) agreed well with time-resolved measurements.

**Keywords:** Emission spectroscopy, Bayesian, Spark discharge, Plasma, Plasma in liquid

## 1. Introduction

Discharge with liquids is a growing research field with great potential not only in applications, such as nanomaterial synthesis [1], water sterilization, and medicine [2], but also in fundamental (plasma) physics. Plasma can be coupled to a liquid in various configurations (in-liquid, in-contact with liquid, in gaseous bubbles, or in gas with liquid droplets), and various discharge modes can be sustained, such as glow, streamer, spark, etc. [3]. Herein, we focus on in-liquid spark discharges that showed interest in the field of nanomaterial synthesis [1]. For instance, discharges between metal electrodes in water produce metal oxide nanoparticles such as CuO, $Cu_2O$, NiO, CoO, $Al_2O_3$, etc. [1, 4, 5], while discharges between metal electrodes in liquid hydrocarbons produce nanocomposite materials, i.e. metal nanoparticles embedded in a hydrogenated C-matrix [6].

In-liquid spark discharge is a fast and transient phenomenon characterised by a high electrical current (~10-100 A), high initial pressure (~10-100 bar), high temperature (5,000-10,000 K), emission of shock waves, and formation of bubbles. The high intensity of the emitted radiation in the visible range allows its characterization by optical emission spectroscopy [7]. However, its transient [1] and stochastic nature [8] makes the application of such a diagnostic technique a challenge. The plasma evolves rapidly (~ ns), which suggests that integration periods of the optical acquisition device should be in the same order (ns). Although it is technologically feasible, the stochastic nature of the discharge occurrence makes it useless, and integration periods around 10-50 ns are more adapted. Moreover, as the discharge modifies the electrode (via erosion) and the liquid composition (dissociation and enrichment with nanoparticles) continuously, the plasma properties change with time. In these conditions, the coherence of the acquired spectra and the derived characteristics become questionable. An alternative way to overcome the difficulties related to stochasticity and non-reproducibility lies in the acquisition of time-integrated spectra. However, the challenge becomes the interpretation of the spectra and the determination of time-dependent plasma properties.

The goal of this work is to evaluate the utilization of a Bayesian method in the analysis of optical emission spectra. This method is widely used in the exploitation of astrophysical data [9], but not yet to a laboratory plasma. The advantages of a Bayesian method are numerous. For instance, it can be applied to datasets with considerable noise, and reliable properties can be obtained. Moreover, it provides information on the possible correlation between different parameters, i.e. relationships between them.

In this paper, we explore the potential of the Bayesian method in the exploitation of a time-integrated optical emission spectrum of a spark discharge in water. This study case was chosen because of the transient nature of the discharge and, more particularly, because of the non-conclusive interpretation of such spectra in literature. In this first approach, we focus the development of the model for Hα line profile and intensity, and later an analysis of the complete spectrum will be performed.

## 2. Conditions of data acquisition

The optical emission spectra are acquired using the same experimental setup as in [10]. Briefly, the discharge was generated between two copper electrodes immersed in 100 mL of distilled water. The interelectrode gap distance was set to 100 µm. The high-voltage pulses (at 20 kV amplitude and 500 ns pulse width) was provide by a power supply (NSP 120-20-P-500-TG-H) from Eagle Harbor Technologies. Acton 2750 spectrometer (equipped with a grating of 300 lines/mm) coupled to an ICCD camera (PI-MAX) from Princeton instruments were utilized to acquire the optical emission spectra from 300 to 900 nm. The time-integrated spectra were acquired at 1 µs exposure time, while the time-resolved spectra were acquired at 50 ns exposure time. The synchronization between the high-voltage pulse and the ICCD camera was ensured using an external pulse generator (Quantum Composers Plus 9518).

## 3. Results and discussion

### 3.1. Conventional processing of the experimental data

Fig. 1 shows a typical spectrum that is averaged over space and time (exposure time of 1 µs). Clearly, it contains many information, such as continuum component that could be attributed to a blackbody radiation (~5,000-7,000 K), emission of $H_\alpha$ at ~656 nm (and absence of $H_\beta$ and other H lines), and emission of O at ~777 and 844 nm. Although

different information can be derived from such a spectrum, we will focus on Hα line, as mentioned earlier.

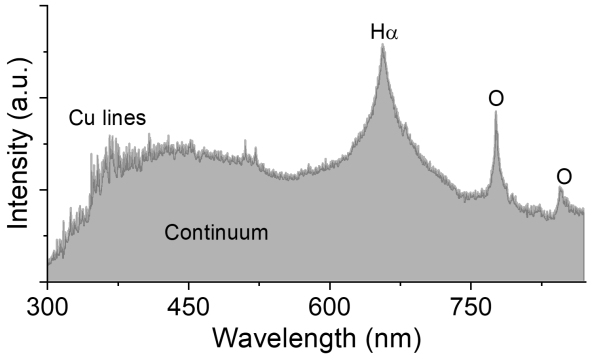


Fig. 1. 1-μs-integrated optical emission spectrum from 300 nm and 900 nm for in-water spark discharge.

The profile of a line is often utilized to determine some plasma parameters, such as electron density ($n_e$). Here, Hα line profile will be utilized to determine $n_e$. At this stage, it is worth reminding that the presence of different sources of broadening contributes to the measured profile, namely experimental, Doppler, natural, resonant, Van der Waals, and Stark broadenings. Experimental and Doppler broadenings have Gaussian profile, while the others have Lorentzian profile. Considering typical conditions for in-liquid spark discharge [7, 11, 12], i.e. $n_e$ ~$10^{25}$ $m^{-3}$, $T$ ~5,000 K, and $P$ ~100 bar, one can estimate the broadening (FWHM, Full Width at Half Maximum) provided by each source [13]; the values are summarized in Table 1.

Table 1. Different broadenings of the Hα line calculated for $n_e = 10^{25}$ $m^{-3}$, $P$ = 100 bar, and $T$ = 5,000 K.

| Sources | Gaussian; Δλ (nm) | Lorentzian; Δλ (nm) |
|---|---|---|
| Experimental | 0.07 | - |
| Doppler | 0.03 | - |
| Natural | - | 0.000117 |
| Resonant | - | 0.1 |
| Van der Waals | - | 0.52 |
| Stark | - | 17.95 |

The different broadening values reported in Table 1 clearly show a dominance by Stark broadening. The measured profile convolutes Gaussian and Lorentzian broadening, and results in a Voigt profile. Considering the known broadenings, Hα line (extracted from Fig. 1 and background-corrected by a linear baseline correction, i.e. the continuum radiation is considered linear in the range of 550-750 nm) is fitted by a Voigt profile, and the best obtained fit is shown in Fig. 2. Clearly, one remarks that the Voigt profile is far to represent the measured profile. The failure is principally due to the fact that the integrated spectrum is a sum of different profiles, with different amplitudes and broadenings.

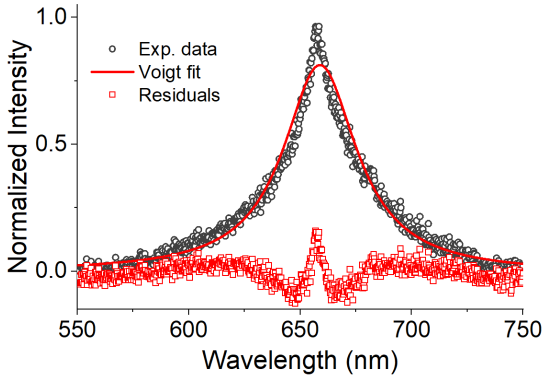


Fig. 2. 1-μs-integrated Hα profile and its fit with a Voigt profile.

### 3.2. Bayesian method and model description

The application of a Bayesian method in the fit of the integrated experimental Hα line profile necessitates the establishment of a deterministic model based on some physical assumptions. The model considered here is the description of the light profile, $I_{light}(\lambda)$, in optically-thin plasma conditions:

$$I_{light}(\lambda) = C_1 \left( \int_0^{1\,\mu s} f(t)\, P_{Lor}(\lambda, t)\, dt \right) + (A\lambda + B) \quad (1)$$

$C_1$ is a constant (to consider the solid angle of detection from the optical fiber and the sensitivity of the ICCD camera). In Equation (1), $f(t)$ accounts for temporal variations of the density of the emitting level. Assuming Boltzmann distribution for hydrogen excited states, $f(t)$ can thus be linked to temporal variations of the ground-state hydrogen population and excitation temperature. In Equation (1), $A$ and $B$ are linear baseline correction parameters. As for $P_{Lor}(\lambda, t)$, it corresponds to the unity-normalized Lorentzian line profile:

$$P_{Lor}(\lambda, t) = \frac{1}{1 + \left( \frac{\lambda - \lambda_0}{\Delta\lambda(t)} \right)^2} \quad (2)$$

where $\Delta\lambda(t)$ is the line broadening at $t$, and $\lambda_0$ is the center of the line. We consider in the model that broadening only results from the Stark effect. Besides, only the linear stark effect is considered. In this condition, Stark broadening is linked to the electron density, $n_e$, through [14]:

$$\Delta\lambda_{Stark}[nm] = 8.33 \times 10^{-3} \left( \frac{n_e[m^{-3}]}{10^{20}} \right)^{\frac{2}{3}} \quad (3)$$

At this stage, one needs to propose a model to describe the temporal evolution of $n_e$. Previous studies on this subject suggest that an exponential decay may be accepted [7, 12, 15]. Therefore, we chose to represent $n_e(t)$ by:

$$n_e(t) = n_{e0} \exp\left(-\frac{t}{\tau_e}\right) \quad (4)$$

where $n_{e0}$ is the electron density at the beginning of the discharge, and $\tau_e$ is the characteristic temporal decay time.

Dynesty Python package was used to implement the Bayesian method [17, 18, 19]. A nested sampling method was also used to evaluate the posterior distribution of the set of parameters with a combination of static and dynamic sampling with 2,500 live points and multiple bounding ellipsoid condition. The logarithm of the likelihood $L(\Theta)$ is expressed as in equation (6):

$$L(\Theta) = -\frac{1}{2}\sum_{i=1}^{N_{obs}} \left( \frac{I_{light}(\lambda_i, \Theta) - I_{data}(\lambda_i)}{\sigma_i} \right)^2 \quad (6)$$

$\Theta$ is the vector of all the parameters, $I_{data}(\lambda_i)$ is the experimental data, $\sigma_i$ is the standard deviation of the experimental data (set to 0.15), and $N_{obs}$ is the number of data points (set to 3,610). To compute the integral of equation (1), 200 discrete time steps of 5 ns are used. The lower and higher limits of the parameters are listed in Table 2 and are used to define the uniform prior distribution. In these conditions, Python program chooses randomly numerous sets of parameters and evaluates the likelihood of each one. Then, for the regions in the parameter domain with the highest probability, more samples will be tested until a convergence criterion [17] is reached. Finally, the set of parameters is provided (best values in Table 2) in addition to the profile predicted by the model (Fig. 3).

Table 2. Summary of the parameters, the lower and higher limits, and the best values with 95% certitude interval.

| Parameters | Lower limit | Higher limit | Best values |
|---|---|---|---|
| $\tau_e\ [ns]$ | 1 | 1000 | $136^{+29}_{-54}$ |
| $\log_{10}(n_{e0}\ [m^{-3}])$ | 20 | 27 | $25.8^{+1}_{-1.1}$ |
| $\lambda_0\ [nm]$ | 640 | 670 | $658.3^{+0.3}_{-0.3}$ |
| $A\,.\,10^{-4}$ | $-100$ | 100 | $-6.5^{+8}_{-8}$ |
| $B$ | $-1$ | 1 | $-0.044^{+0.053}_{-0.053}$ |

Fig 4. compares the measured $H_\alpha$ profile and the fit predicted by the model using the parameters summarized in Table 2. Clearly, the agreement between these two profiles is much higher than that obtained from the Voigt fit, presented earlier (Fig. 3).

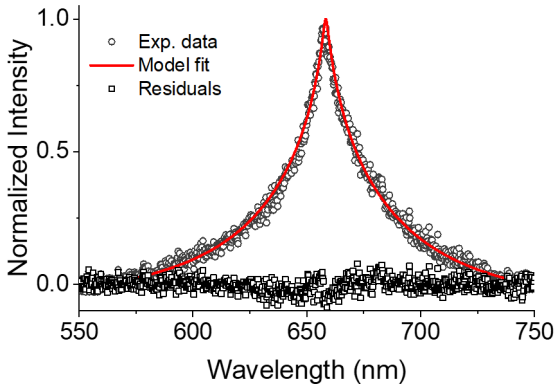


Fig. 3. 1-µs-integrated Hα profile and its fit using Bayesian method with the parameters in Table 2.

To evaluate the model accuracy, time-resolved emission spectra are acquired with an exposure time of 50 ns. We used Lorentzian profile to fit the profiles of the two lines, $H_\alpha$ and O (at 777 nm), to determine $n_e(t)$ [20]. Fig. 4 shows the normalized experimental spectrum of the $H_\alpha$ line and the corresponding Lorentzian fit at different moments in the discharge.

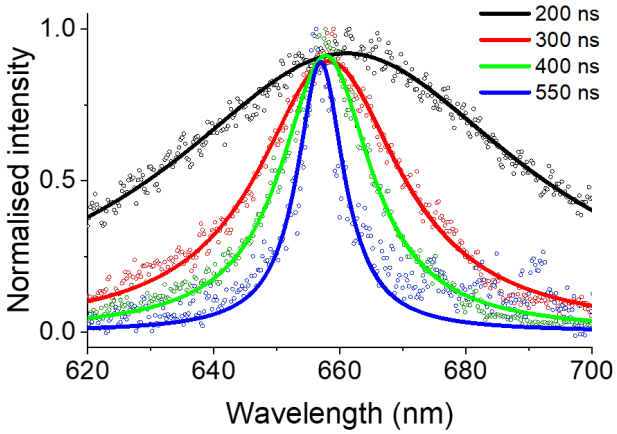


Fig. 4. 50-ns-integrated Hα profile and its fit with a Voigt profile at different moments in the discharge.

Finally, we present in Fig. 5 the temporal evolution of $n_e(t)$ (with uncertainty) predicted by the model, and added to the values measured at different moments. Except the datapoint at 200 ns, a great agreement between the two data sets, both in magnitude and characteristic time, is observed. Moreover, it is worth noting that the characteristic time of the exponential decay found here (~136 ns) is comparable with that determined in other studies (~100 - 200 ns) under similar in-liquid discharge conditions [7, 15]. As for the measurement of the $n_e$ at 200 ns, which does not agree with the model prediction, we believe that the Lorentzian fit may not be adapted. Indeed, $H_\alpha$ line can have a strong self-absorption, and this has not been considered in the Lorentzian fit. In fact, we performed a fit of this profile while considering the self-absorption, and the determined value (back star in Fig. 5) agrees well with the prediction

of the model. This finding suggests that self-absorption should be considered in the model, and this will be performed in a future study.

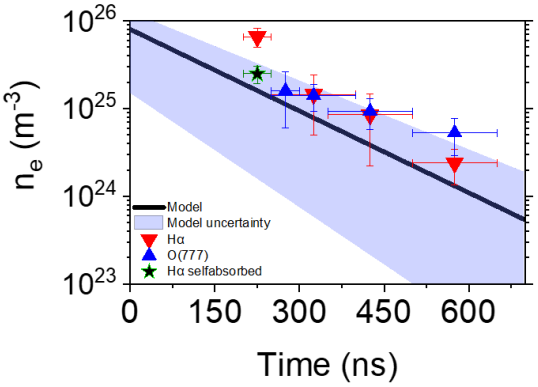


Fig. 5. Temporal evolution of $n_e$ predicted by the model, and the $n_e$ values determined by Lorentz fit of 50-ns-integrated Hα and O line profiles.

## 4. Conclusions and perspectives

In this work, we explore the potential of the Bayesian method in the exploitation of optical emission spectra of in-liquid spark discharges. We showed that it is not feasible to fit an integrated spectrum with a Voigt profile, because it does not consider the temporal evolution of plasma properties, i.e. profile amplitude and broadenings. However, the use of Bayesian method while considering a simplified model provided a very good agreement between the measured and the predicted profiles. The model assumed an exponential delay of $n_e$, and the predicted values of $n_e$ and the characteristic time perfectly agrees with the reported measurements in literature. The method was validated by reporting $n_e$ at different moments in the discharge using time-resolved emission spectra. Finally, we believe that Bayesian method could play a useful role in the processing of optical emission spectra, and a more complete model to describe the whole spectrum while considering other phenomena (continuum, absorption, etc.) showed is under development.

## 5. Acknowledgements

This research was funded by the Natural Sciences and Engineering Research Council of Canada (NSERC). The authors thank the Fonds de Recherche du Québec—Nature et Technologie (FRQ-NT) and the Canada Foundation for Innovation (CFI) for funding the research infrastructure.

## 6. References

[1] T. Belmonte et al., *J. Phys. D. Appl. Phys.*, 47, (2014).
[2] I. Levchenko *et al.*, *Appl. Phys. Rev.*, 5, (2018).
[3] P. Bruggeman and C. Leys, *J. Phys. D. Appl. Phys.*, 42, (2009).
[4] A. Hamdan et al. *Plasma Chem. Plasma Process.*, 41, 433–445 (2021).
[5] T. Merciris et al. *J. Appl. Phys.*, 129, 063303, (2021).
[6] X. Glad et al. *Sci. Rep.*, 11, 1–12, (2021).
[7] T. Belmonte et al., *Plasma Sources Sci. Technol.*, 27, (2018).
[8] N. Bourbeau et al. *J. Phys. D. Appl. Phys.*, 54, (2021).
[9] B. Benneke and S. Seager, *Astrophys. J.*, 753, (2012).
[10] T. Merciris et al. *IEEE Trans. Plasma Sci.*, 48, (2020).
[11] A. Hamdan et al. *J. Acoust. Soc. Am.*, 134, 991–1000, (2013).
[12] A. Von Keudell et al., *Plasma Sources Sci. Technol.*, 29, (2020).
[13] T. Belmonte et al. *Plasma Sources Sci. Technol.*, 24, (2015).
[14] I. Marinov et al., *J. Phys. D. Appl. Phys.*, 47, (2014).
[15] A. Hamdan et al., *Plasma Chem. Plasma Process.*, 34, 1101–1114, (2014).
[16] R. D. Cowan and G. H. Dieke, *Rev. Mod. Phys.*, 20, 418–455, (1948).
[17] J. S. Speagle, *Mon. Not. R. Astron. Soc.*, 493, 3132–3158, (2020).
[18] F. Feroz et al., *Mon. Not. R. Astron. Soc.*, 398, 1601–1614, (2009).
[19] E. Higson et al. *Stat. Comput.*, 29, 891–913, (2019).
[20] T. Maehara *et al.*, *Phys. Plasmas*, 16, 1–6, (2009).